Journal of ETA Maritime Science 2022;10(4):223-236

Crossover Operators in a Genetic Algorithm for Maritime Cargo Delivery Optimization

Vadim V. Romanuke, Andriy Y. Romanov, Mykola O. Malaksiano

Odessa National Maritime University, Department of Technical Cybernetics and Information Technologies, Odessa, Ukraine

Abstract

Maritime cargo delivery accounts for over 80% of the world's trade and contributes about 3% of the world's gross domestic product. Here, we focus on the problem of minimizing the maritime cargo delivery cost by an amount equivalent to the sum of the tour lengths of feeders used for the delivery. We formulate maritime cargo delivery cost reduction as a multiple traveling salesman problem and use a genetic algorithm to solve it. In addition to minimizing the route length, the algorithm indirectly reduces the number of feeders. To increase the performance of the genetic algorithm, we implement a 3-point crossover operator, which takes three chromosomes and returns slightly more complex crossover mutations than the known 2-point crossover operator. These two operators must be used in confluence. We propose to run both the 2-point crossover algorithm and the 2-point-and-3-point crossover algorithm in parallel and select the route with the shortest length. The route length is cut down by a few percent, which makes a big difference in how much it costs to ship cargo by sea.

Keywords: Maritime cargo delivery, Tour length, Genetic algorithm, Crossover

1. Introduction

Maritime transportation is the basis of the world trade and commerce. Approximately 80% of all goods are transported by river, sea, and ocean. The global cargo shipping market was valued at $11.36 billion in 2021, and it is expected to reach $16.43 billion by 2029. This corresponds to a compound annual growth rate of 4.72% during the forecast period of 2022-2029 [1]. According to United Nations Conference on Trade and Development [2], shipping is responsible for more than 80% of the globe's trade, and the total contribution of the industry to the global economy is estimated at 3% of the globe's gross domestic product. In addition to the market insights such as market value, growth rate, market segments, geographical coverage, market players, and market scenario, the market report supported by the Data Bridge Market Research team also includes in-depth expert analysis, import/export analysis, pricing analysis, production consumption analysis, and PESTLE (PESTLE stands for political, economic, social, technological, legal, and environmental) analysis [3].

The maritime delivery market is divided into regions, each of which represents an important part of the entire market. The Mediterranean Sea is an important maritime and commercial route, containing 87 ports of various sizes and strengths servicing local, regional, and international markets. The Asia-Pacific region is considered the manufacturing hub for automotive companies. Regionally and globally, China holds the largest market share for cargo shipping. There are 34 major and more than 2000 minor ports in China. All the 926 ports in the United States are essential to the nation's competitiveness, as 99% of overseas trade travels through them. The Middle East and Africa are also expected to show augmented growth in the market. Improved port connections and a greater emphasis on modernizing and expanding existing ports have boosted the amount of trade in this region [4].

A. P. Moller-Maersk [5], Mediterranean Shipping Company [6], China COSCO Shipping [7], and CMA CGM Group [8] are the key players whose market share in terms of deployed capacity exceeds 10%. Hapag-Lloyd, ONE, Evergreen, Yang

Address for Correspondence: Vadim V. Romanuke, Odessa National Maritime University, Department of Technical Cybernetics and Information Technologies, Odessa, Ukraine
E-mail: romanukevadimv@gmail.com
ORCID ID: orcid.org/0000-0003-3543-3087

Received: 06.07.2022
Last Revision Received: 07.10.2022
Accepted: 12.10.2022

To cite this article: V.V. Romanuke, A.Y. Romanov, M.O. Malaksiano, "Crossover Operators in a Genetic Algorithm for Maritime Cargo Delivery Optimization." *Journal of ETA Maritime Science*, vol. 10(4), pp. 223-236, 2022.

Ming, Pacific International Lines, and Hyundai [2] complete the top 10 deep-sea container shipping lines, with a market share greater than 2% (but less than 9%; the shipping lines are listed in descending order). According to the review of maritime transport, published by the United Nations Conference on Trade and Development in 2019, three major alliances account for nearly 87% of the cargo shipped on the transpacific route, 98% of the Asia-Europe trade, and about 80% of the containership capacity deployed globally [2].

Cargo shipping is a means of transportation used to convey commodities, goods, cargo, etc., from a seaport to a destination through vessels, cargo ships, and others. Shipping is the cheapest means of transportation per ton. It is preferred due to its economic and environmental friendliness in long-distance transportation. Increasing orders for the import/export of manufactured goods, the transportation of raw materials in bulk, and affordable food items fuel the demand for waterborne freight transportation. The expansion of the global supply chain, the liberalization of trade policies, and technological advancement in waterborne shipping have propelled the trade of intermediate and manufactured products and significantly reduced coordination and transportation costs. To maximize the potential of maritime transportation, it is necessary to plan efficient tours. Typically, a tour consists of one or more hubs, which serve as a starting point, and many ports, which function as local destinations for cargo delivery. A route comprised of tours should be divided as rationally as possible between feeder ships (medium-sized freight ships) and route-based tours (having a minimal length and being covered by a minimal number of feeders). The efficient tour has the smallest length possible, expressed in either distance or time units (or both). Minimizing the tour length is a transportation optimization problem [9]. This is a version of the traveling salesman problem applicable to cargo shipping [10], where feeder ships must be freighted at the hub, deliver their cargo, and return to the hub (in addition, they can be re-freighted with cargo at some ports heading toward the hub). Recent studies have investigated different approaches to solving this problem, including deterministic, meta-heuristic, and market-based approaches [9,11]. However, heuristic-based approaches that offer greater advantage in computational efficiency are the cutting edge in rational routing [12]. Only a few exact method approaches have been introduced in recent years [13]. Therefore, heuristics with their combinations (metaheuristics) and extensions (matheuristics) are typically sufficient for route optimization tasks.

2. Literature Overview and Motivation

An exact solution to the traveling salesman problem routes efficient tours. Such routing minimizes the cost of maritime delivery. The traveling salesman problem is an NP-hard problem in combinatorial optimization [14]. An exact solution to the traveling salesman problem usually takes too long to be obtained because an exact algorithm performs reasonably fast only for small-sized problems [15]. Finding the exact solution becomes exponentially intractable as the number of ports (sometimes referred to as cities) is increased, starting with a few tens [11,14]. Heuristic algorithms produce approximate solutions far more quickly. The difference between an approximate solution and an exact solution is usually acceptable [12,16]. It is highly probable that an approximate solution given by a heuristic is at most 3% away from the optimal solution, even for large routing problems (with thousands of ports and cities) [11,17]. Meanwhile, heuristic algorithms immensely save computational resources equivalent to operational time [14,15]. Rerouting maritime delivery tours when it is urgent has a significant economic impact.

The genetic algorithm is one of the greatest heuristics since it allows for the discovery of tours whose length is practically close to the minimal length of the delivery [17,18]. Usually, it is faster than the algorithms of ant colony optimization, simulated annealing, and tabu search while maintaining the same accuracy [9,14,19]. For maritime cargo delivery using multiple tours covered by multiple feeder ships, the genetic algorithm inputs are a map of ports, a number of feeders, a population size, mutation operators, and a series of additional minor parameters. The map of ports is the two-coordinate location of ports that should be visited en route. The number of feeders defines the maximum number of tours by which the cargo can be delivered. The population size is the number of randomly generated tours to be processed by the algorithm. The mutation operators are intended to occasionally break one or more members of a population out of the local minimum space and potentially discover a better minimum space.

The crossover is a convergence operation designed to pull the population toward a local minimum [18,20]. The majority of genetic algorithms use single-point crossovers. Single-point crossover is a technique where the selected parent population, i. e., the two mating chromosomes, is cut at a randomly selected location known as the pivot point or crossover point. At this cut, the genetic information to the left (or right) of the point is swapped between the two parent chromosomes to produce two offspring chromosomes (children). This technique becomes more robust if each parent has its own pivot point. These pivot points are also selected at random. Then it is a 2-point crossover mutation, although it is sometimes still referred to as a single-point crossover (due to every parent is cut at a single point) [17,18,21]. A 2-point crossover mutation increases

performance of the genetic algorithm by accelerating convergence and shortening route lengths. Therefore, it may be expected that a more complex operation of crossover mutations can result in an even greater performance boost.

Therefore, the goal is to try a more complex crossover mutation to improve the performance of the genetic algorithm. This is believed to have a significant impact on the future rationalization of maritime transportation route design to improve maritime cargo shipping and delivery. To achieve the goal, the following six tasks need to be fulfilled:

1. Introduce and explain the variables and denotations used in the genetic algorithm for a maritime cargo delivery model.

2. Formalize the genetic algorithm using 2-point crossover mutations.

3. Suggest a more complex operation of crossover mutations based on the fact that multiple feeders are used for maritime cargo delivery.

4. Evaluate how the algorithm with the suggested crossover mutation operation performs in comparison with the known 2-point crossover mutation operation.

5. Explore the practical applicability and significance of the suggested crossover mutation operation in the genetic algorithm.

6. Conclude on the contribution to the field of genetic algorithms used in optimizing maritime cargo delivery. Outline a possible extension of the research.

The rest of this paper is organized as follows: A model of maritime cargo delivery is presented in Section 3. Section 4 formalizes a genetic algorithm using a 2-point crossover mutation operator. The 2-point crossover mutation is additionally explained with a visual example. Section 5 introduces our 3-point crossover mutation operator, accompanied by a visual illustration of the 3-point crossover mutation. The testing results for both 2-point and 3-point crossover operators are presented and analyzed in Section 6. Our contribution is discussed in Section 7, whereupon we conclude with the main findings in Section 8.

3. Maritime Cargo Delivery Model

Denote by N a number of ports, from one of which every feeder starts its tour and ends up by returning to that port. By default, the port is assigned number 1 and is called the hub. The positions or coordinates of all N ports are known. These positions are naturally presumed to be flat because no ship can ascend or descend. For port k, denote them by p_{k1} (the horizontal position) and p_{k2} (the vertical position). Positions of all the ports are gathered in matrix

$$\mathbf{P}=\left[p_{kl}\right]_{N\times 2}. \tag{1}$$

It is assumed that if a feeder must go from port k to port j, without additional stops, then the feeder accomplishes it in a straight line. Therefore, the distance covered by the feeder from port k directly to port j (or in the opposite direction) is

$$\rho(k,j)=\sqrt{\left(p_{k1}-p_{j1}\right)^2+\left(p_{k2}-p_{j2}\right)^2}=\rho(j,k)$$

by $k=\overline{1,N}$ and $j=\overline{k+1,N}$. (2)

Formally,

$$\rho(k,k)=0 \quad \forall k=\overline{1,N}. \tag{3}$$

It is quite natural to assume that the speed of every feeder heading for a port is (roughly) constant.

Then these $\frac{N(N-1)}{2}$ non-zero distances

$$\left\{\left\{\rho(k,j)\right\}_{k=1}^{N}\right\}_{j=k+1}^{N} \tag{4}$$

in (2) can be easily mapped into durations of the maritime cargo delivery. The durations can be subsequently mapped into the respective costs of the delivery. The general aim is to minimize such costs.

Denote by $M_{\max}$ the number of feeders available to accomplish the delivery. Usually, there are at least two available feeders. Hence, $M_{\max}\in\mathbb{N}\setminus\{1\}$. However, an additional aim is to enable as less feeders as possible.

If feeder m visits either port j after port k or port k after port j (the direction here does not matter), then this fact is featured with a flag: $x_{kjm}=1$. To exclude repeated flags in the case when feeder m visits more than one port (apart from the hub), we assign $x_{jkm}=0$ if $x_{kjm}=1$ and $x_{kjm}=0$ if $x_{jkm}=1$. When feeder m leaves the hub to visit only port k and then returns to the hub, we assign $x_{1km}=x_{k1m}=1$. If feeder m does not visit port j after port k nor port k after port j, then $x_{kjm}=0$ (although ports k and j still can be included into the tour of feeder m). So, each flag

$$x_{kjm}\in\{0,1\} \text{ by } k=\overline{1,N} \text{ and } j=\overline{1,N} \text{ and } m=\overline{1,M} \tag{5}$$

by a (current) number of feeders M, where $M\leqslant M_{\max}$. Henceforward, we have two first constraints. First, each of M feeders only once departs from the hub:

$$\sum_{j=2}^{N}\sum_{m=1}^{M}x_{1jm}=M. \tag{6}$$

Second, each of M feeders only once arrives at the hub:

$$\sum_{k=2}^{N}\sum_{m=1}^{M}x_{k1m}=M. \tag{7}$$

Only one feeder can arrive at port j, being not the hub, from only one port (which can be the hub). This constraint is expressed by an equality

$$\sum_{k=1}^{N}\sum_{m=1}^{M}x_{kjm}=1 \quad \forall j=\overline{2,N}. \tag{8}$$

Symmetrically, only one feeder can depart from port k, being not the hub, toward only one following port (which can be the hub). This constraint is expressed by an equality

$$\sum_{j=1}^{N}\sum_{m=1}^{M} x_{kjm} = 1 \quad \forall k = \overline{2, N}\,. \tag{9}$$

In addition to constraints (6)-(9), any subtour of a feeder should be eliminated with the following requirement:

$$\sum_{k\in Q_m}\sum_{j\in Q_m\setminus\{k\}} x_{kjm} \leqslant |Q_m| - 1$$

$$\forall Q_m \subset T_m \subset \left\{\overline{1, N}\right\} \text{ by } 2 \leqslant |Q_m| < A_m \text{ and } \forall m = \overline{1, M} \tag{10}$$

with tour

$$T_m = \left\{1, \left\{q_l^{(m)}\right\}_{l=2}^{A_m}\right\} \subset \left\{\overline{1, N}\right\} \tag{11}$$

of feeder m. The inequality in (10) means that if Q_m is a subtour of tour (11), then its ports are not connected into a closed loop owing to fact that at least one pair of ports are disconnected (it is that term $|Q_m| - 1$). Constraint (10) with (11) ensures that every feeder has a tour as a closed loop: it departs from the hub and arrives at it. Owing to this constraint, a feasible route of delivering maritime cargo is of closed loops only, where every loop is a feeder tour that starts at the hub and ends by returning to the hub.

The sixth constraint is determined by the capacity of the feeder fleet. Obviously, the feeder has a limit on the distance it can cover without a fuel refill. Denote this limit by $d_{\max}$. Therefore, inequality

$$\sum_{k=1}^{N}\sum_{j=1}^{N} \rho(k, j)\cdot x_{kjm} \leqslant d_{\max} \quad \forall m = \overline{1, M} \tag{12}$$

constraints the tour of every feeder. Herein, nevertheless, we do not define the shortest possible tour of the feeder. If a feeder is enabled for delivery, it must (and definitely will) visit at least one port, not the hub.

To optimize maritime cargo delivery, the sum of all the tours of the feeders is to be minimized. The respective objective function

$$\rho_{\Sigma}\left(N, M, \left\{\left\{\left\{x_{kjm}\right\}_{k=1}^{N}\right\}_{j=1}^{N}\right\}_{m=1}^{M}, d_{\max}\right) =$$

$$= \sum_{k=1}^{N}\sum_{j=1}^{N}\sum_{m=1}^{M} x_{kjm}\cdot\rho(k, j) \tag{13}$$

is to be minimized subject to flags (5) and constraints (6)-(12). The minimization is implied to be done over binary variables (5), along with trying to minimize the total number of feeders used in the tours. That is, the minimization objective is to find such

$$M^* \in \left\{\overline{1, M_{\max}}\right\} \tag{14}$$

and

$$x_{kjm}^* \in \{0, 1\} \text{ for } k = \overline{1, N} \text{ and } j = \overline{1, N} \text{ by } m = \overline{1, M^*} \tag{15}$$

at which

$$\sum_{k=1}^{N}\sum_{j=1}^{N}\sum_{m=1}^{M^*} x_{kjm}^*\cdot\rho(k, j) =$$

$$= \rho_{\Sigma}\left(N, M^*, \left\{\left\{\left\{x_{kjm}^*\right\}_{k=1}^{N}\right\}_{j=1}^{N}\right\}_{m=1}^{M^*}, d_{\max}\right) =$$

$$= \min_{\substack{\left\{\left\{x_{kjm}\right\}_{k=1}^{N}\right\}_{j=1}^{N}, \\ m=\overline{1, M}, M=\overline{1, M_{\max}}}} \sum_{k=1}^{N}\sum_{j=1}^{N}\sum_{m=1}^{M} x_{kjm}\cdot\rho(k, j)\,. \tag{16}$$

The solution given formally as

$$\left\{\left\{\left\{x_{kjm}^*\right\}_{k=1}^{N}\right\}_{j=1}^{N}\right\}_{m=1}^{M^*} \tag{17}$$

allows building a set of M^* the most rational tours of M^* feeders. Sum (16) of these tours is the length of the shortest route to deliver maritime cargo and return to the hub. Nevertheless, the solution to this problem may not be unique. For example, there may be two shortest routes (whose lengths are equal), but one of them can be covered with a lesser number of feeders. Then the route covered by such feeders is usually accepted. An additional criterion to select a route should be formulated if both the shortest routes are covered by the same number of feeders.

4. Algorithm Using 2-point Crossover

There are usually at least a few tens of ports for delivery, so exact methods are intractably time-consuming to find minimal-length routes. The computational task is thus simplified to finding a route whose length is practically close to the shortest route length. An approximately minimal-length route is obtained by a genetic algorithm specifically designed for solving problem (16) subject to flags (5) and constraints (6)-(12) [20]. The primary steps of the algorithm are the random population generation, the currently best result evaluation, and mutations.

Let H_m be the number of ports that feeder m should visit after starting off port 1 (the hub), whereupon the feeder returns to the hub (so, the hub is not counted in this number). Consider a vector of ports that feeder m should visit in the order of the sequence of the vector elements (apart from the hub). So, this vector

$$\mathbf{F}_m = \left[f_h^{(m)}\right]_{1\times H_m} \tag{18}$$

is a tour of feeder m. Tours $\{\mathbf{F}_m\}_{m=1}^{M}$ of all feeders constitute a route of delivery (apart from the hub). This means that

$$\bigcup_{m=1}^{M}\left\{f_h^{(m)}\right\}_{h=1}^{H_m} = \left\{\overline{2, N}\right\} \tag{19}$$

due to

$$\left\{\overline{2, N}\right\} \tag{20}$$

is the set of all non-hub ports.

Before the genetic algorithm runs into the first iteration, tours $\{\mathbf{F}_m\}_{m=1}^{M}$ of feeders are randomly generated by breaking the set of non-hub ports (20). Each feeder has a series of such tours called chromosomes. Altogether, such a series of all the feeders constitute a population. Each element of the population is a route of delivery using M feeders represented as M respective chromosomes. For every route of the population, the following routine is executed during an iteration of the algorithm. First, the distance to the port following the hub is calculated as

$$d_m = \rho\left(1, f_1^{(m)}\right) . \tag{21}$$

Then, the remaining distances except the last one are accumulated into d_m:

$$d_m^{(\text{obs})} = d_m , \;\; d_m = d_m^{(\text{obs})} + \rho\left(f_k^{(m)}, f_{k+1}^{(m)}\right)$$

$$\text{for } k = \overline{1, H_m - 1} . \tag{22}$$

Finally, the distance of returning to the hub is:

$$d_m^{(\text{obs})} = d_m \;\; , \;\; d_m = d_m^{(\text{obs})} + \rho\left(f_{H_m}^{(m)}, 1\right) . \tag{23}$$

To improve the selectivity of the best feeder tours, tours that violate condition (12) are expunged. Thus, if $d_m > d_{\max}$ then the current accumulated distance d_m after (23) is increased using a factor $\lambda > 0$:

$$d_m^{(\text{obs})} = d_m \;\; , \;\; d_m = d_m^{(\text{obs})} + \left(d_m^{(\text{obs})} - d_{\max}\right) \cdot \lambda . \tag{24}$$

Finally, sum

$$\tilde{\rho}_{\Sigma}\left(N, M, \{\mathbf{F}_m\}_{m=1}^{M}, d_{\max}\right) = \sum_{m=1}^{M} d_m \geqslant$$

$$\geqslant \rho_{\Sigma}\left(N, M^*, \left\{\left\{\left\{x_{kjm}^*\right\}_{k=1}^{N}\right\}_{j=1}^{N}\right\}_{m=1}^{M^*}, d_{\max}\right) \tag{25}$$

is calculated and minimized over the population to obtain the currently best result. The sum in (25) is the fitness function of the genetic algorithm. A new population is generated based on four forms of chromosome mutation: flip, swap, slide, and crossover [20]. The crossover operator takes two chromosomes (without losing generality)

$$\mathbf{F}_1 = \left[f_h^{(1)}\right]_{1\times H_1} \tag{26}$$

and

$$\mathbf{F}_2 = \left[f_h^{(2)}\right]_{1\times H_2} , \tag{27}$$

whereupon they are either interchanged or merged. This is done using a merging probability P_{merge} given at the input of the genetic algorithm. If $\theta \leqslant P_{\text{merge}}$, where θ is a random value drawn from the standard uniform distribution on the open interval (0;1), then chromosomes (26) and (27) as tours of two different feeders are merged into a single tour:

$$\mathbf{F}_{1\cup 2}^* = \left\{f_h^{(1)}\right\}_{h=1}^{H_1} \cup \left\{f_h^{(2)}\right\}_{h=1}^{H_2} \subseteq \left\{\overline{2, N}\right\} . \tag{28}$$

This allows us to decrease the number of feeders used to deliver maritime cargo. Otherwise, if $\theta > P_{\text{merge}}$ then each chromosome is cut into two random parts. If we leave h_1 first ports in the first chromosome, and h_2 in the second chromosome, the remaining parts are interchanged as follows:

$$\mathbf{F}_1^* = \left[f_h^{(1)*}\right]_{1\times(h_1+H_2-h_2)} = \left(\left\{f_h^{(1)}\right\}_{h=1}^{h_1}, \left\{f_h^{(2)}\right\}_{h=h_2+1}^{H_2}\right) \tag{29}$$

and

$$\mathbf{F}_2^* = \left[f_h^{(2)*}\right]_{1\times(h_2+H_1-h_1)} = \left(\left\{f_h^{(2)}\right\}_{h=1}^{h_2}, \left\{f_h^{(1)}\right\}_{h=h_1+1}^{H_1}\right) . \tag{30}$$

This is a 2-point crossover mutation. An example of a 2-point crossover operation over chromosomes

$$\mathbf{F}_1 = [17 \quad 10 \quad 9 \quad 14 \quad 19 \quad 4 \quad 18 \quad 7 \quad 16 \quad 11]$$

and

$$\mathbf{F}_2 = [2 \quad 8 \quad 15 \quad 6 \quad 5 \quad 12 \quad 3 \quad 13]$$

is shown in Figure 1.

For simplicity, the numbers of chromosomes (26) and (27) are taken as 1 and 2. It does not mean that there are only two feeders left or that only the first two feeders (of $M \geqslant 3$) are subject to crossover mutation. Consequently, if the merging is done by $M \geqslant 3$, single tour (28) is, generally speaking, a part of the route:

$$\mathbf{F}_{1\cup 2}^* \subset \left\{\overline{2, N}\right\} \text{ and } \mathbf{F}_{1\cup 2}^* \neq \left\{\overline{2, N}\right\} .$$

On the contrary,

$$\mathbf{F}_{1\cup 2}^* = \left\{\overline{2, N}\right\}$$

only if M = 2 (i. e., there are two feeders left before the 2-point crossover operation). Therefore, the merged two chromosomes constitute a route of delivery (apart from the hub).

5. 3-point Crossover

If the maritime delivery service can afford to use three feeders or more, the crossover mutation can be made more complex. In this way, three chromosomes are simultaneously mutated by exploiting the interchange pattern of the 2-point crossover operation. In certain cases, determined by random value θ, the three chromosomes are merged into a single tour.

Therefore, in a 3-point crossover mutation, without losing generality, the crossover operator takes three chromosomes (26), (27),

$$\mathbf{F}_3 = \left[f_h^{(3)} \right]_{1\times H_3} \tag{31}$$

whereupon they are either interchanged or merged. If $\theta \leqslant P_{\text{merge}}$ then chromosomes (26), (27), and (31) as tours of three different feeders are merged into a single tour

$$\mathbf{F}^*_{1\cup 2\cup 3} = \left\{ f_h^{(1)} \right\}_{h=1}^{H_1} \cup \left\{ f_h^{(2)} \right\}_{h=1}^{H_2} \cup \left\{ f_h^{(3)} \right\}_{h=1}^{H_3} = \left\{ \overline{2, N} \right\}. \tag{32}$$

Otherwise, if $\theta > P_{\text{merge}}$ then each chromosome is cut into two random parts; having left h_1, h_2, and h_3 first ports in the first, second, and third chromosomes, respectively, the remaining parts are interchanged:

$$\mathbf{F}_1^* = \left[f_h^{(1)*} \right]_{1\times(h_1+H_3-h_3)} = \left\{ \left\{ f_h^{(1)} \right\}_{h=1}^{h_1}, \left\{ f_h^{(3)} \right\}_{h=h_3+1}^{H_3} \right\} \tag{33}$$

and (30) and

$$\mathbf{F}_3^* = \left[f_h^{(3)*} \right]_{1\times(h_3+H_2-h_2)} = \left\{ \left\{ f_h^{(3)} \right\}_{h=1}^{h_3}, \left\{ f_h^{(2)} \right\}_{h=h_2+1}^{H_2} \right\}. \tag{34}$$

An example of the 3-point crossover operation over chromosomes

$$\mathbf{F}_1 = [22 \quad 18 \quad 11 \quad 20 \quad 14 \quad 4 \quad 12],$$
$$\mathbf{F}_2 = [6 \quad 2 \quad 19 \quad 10 \quad 3 \quad 16],$$
$$\mathbf{F}_3 = [5 \quad 7 \quad 8 \quad 9 \quad 23 \quad 15 \quad 13 \quad 21 \quad 17]$$

is shown in Figure 2.

Once again, the numbers of chromosomes (26), (27), and (31) taken as 1, 2, and 3 for the sake of simplicity do not mean that there are only three feeders left at all or that the 3-point crossover operator takes only the first three feeders (of $M \geqslant 4$). If the merging is done by $M \geqslant 4$, single tour (32) is, generally speaking, a part of the route:

$$\mathbf{F}^*_{1\cup 2\cup 3} \subset \left\{ \overline{2, N} \right\} \text{ and } \mathbf{F}^*_{1\cup 2\cup 3} \neq \left\{ \overline{2, N} \right\}.$$

On the contrary,

$$\mathbf{F}^*_{1\cup 2\cup 3} = \left\{ \overline{2, N} \right\} \tag{35}$$

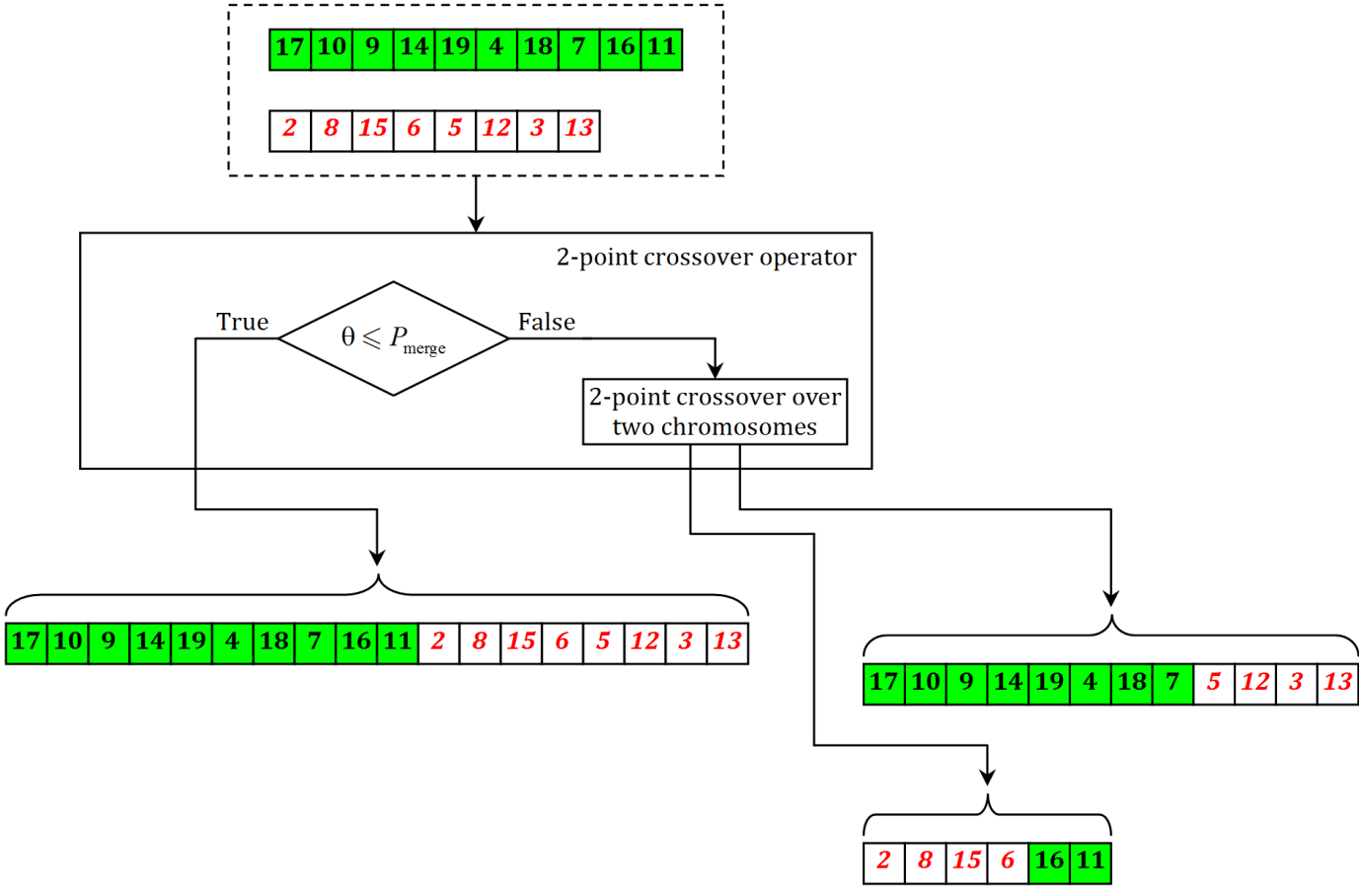

Figure 1. *An example of the 2-point crossover operation over two chromosomes*

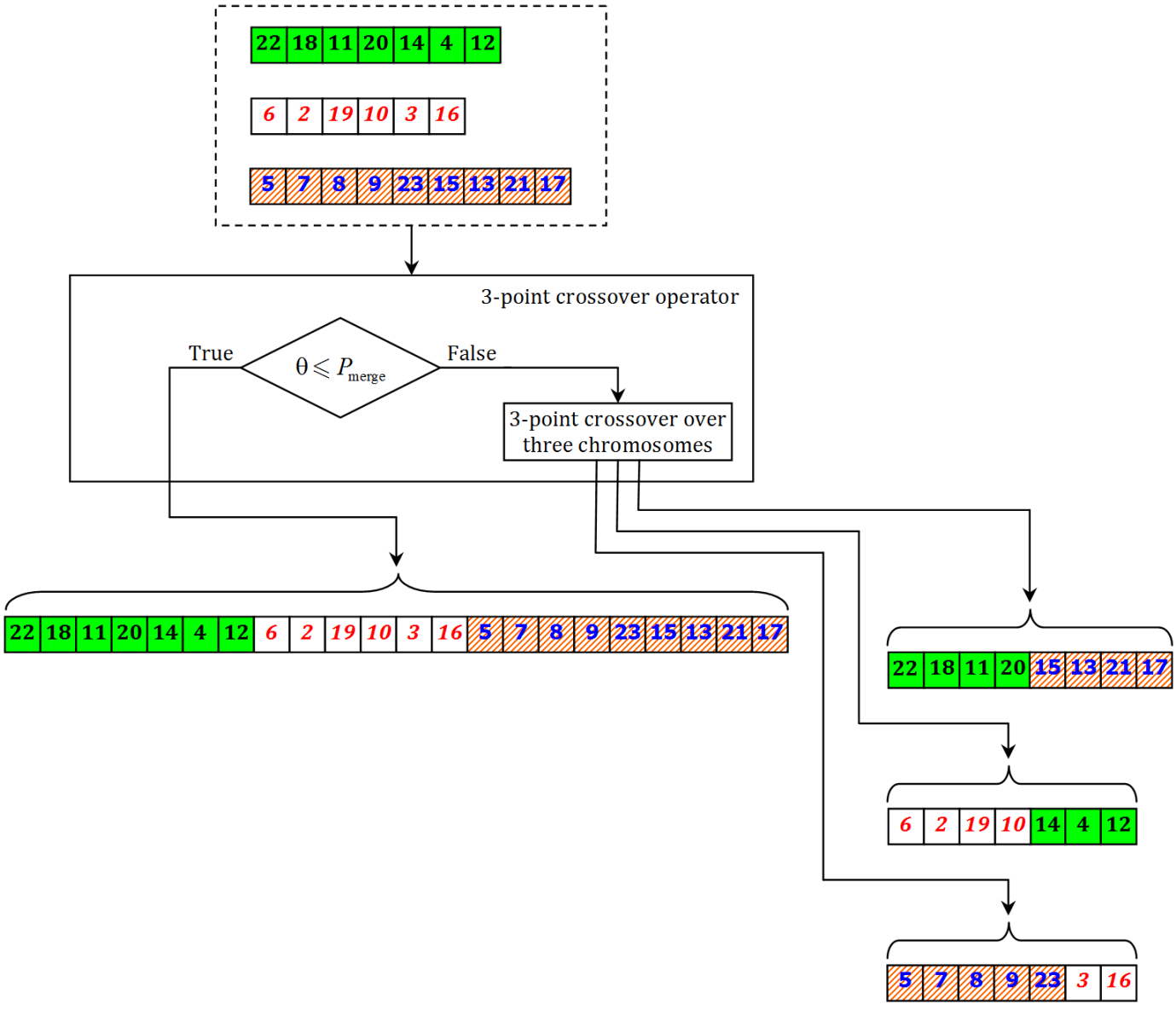

Figure 2. *An example of the 3-point crossover operation over three chromosomes*

only if $M = 3$ (i. e., there are three feeders left before the 3-point crossover operation), so the merged three chromosomes constitute a route of the delivery (apart from the hub). It is easy to see that if $M = 4$ and the 3-point crossover operator merges three chromosomes, then $M = 2$ and further 3-point crossover operations cannot produce a route (35) of a single feeder by the merging. In general, if M (or, before the algorithm starts, $M_{\max}$) is an even number, then the genetic algorithm using only the 3-point crossover operator cannot produce a route of a single feeder.

6. Testing

Denote by $\mu_{2\text{-p}}$ the 2-point crossover operator. This operator is also associated with the corresponding algorithm using it for crossover mutations. Inasmuch as using only the 3-point crossover operator significantly confines the output of the genetic algorithm, we have to test the algorithm using both 2-point and 3-point crossover operators. Denote this algorithm by $\mu_{2,3\text{-p}}$. In fact, algorithm $\mu_{2,3\text{-p}}$ can be thought of as it contains $\mu_{2\text{-p}}$.

Denote by

$$\tilde{\rho}^*_{\Sigma}\left(\mu_{2\text{-p}}\right) = \tilde{\rho}_{\Sigma}\left(N, M^*, \{\mathbf{F}_m\}_{m=1}^{M^*}, d_{\max}; \mu_{2\text{-p}}\right) \tag{36}$$

the shortest route length found by $\mu_{2\text{-p}}$ in $I^*\left(\mu_{2\text{-p}}\right)$ iterations. Length (36) is compared to the shortest route length

$$\tilde{\rho}^*_{\Sigma}\left(\mu_{2,3\text{-p}}\right) = \tilde{\rho}_{\Sigma}\left(N, M^*, \{\mathbf{F}_m\}_{m=1}^{M^*}, d_{\max}; \mu_{2,3\text{-p}}\right) \tag{37}$$

found by $\mu_{2,3\text{-p}}$ in $I^*\left(\mu_{2,3\text{-p}}\right)$ iterations. The percentage

$$g = 100 \cdot \frac{\tilde{\rho}^*_\Sigma\left(\mu_{2\text{-p}}\right) - \tilde{\rho}^*_\Sigma\left(\mu_{2,3\text{-p}}\right)}{\tilde{\rho}^*_\Sigma\left(\mu_{2\text{-p}}\right)} \tag{38}$$

will show either gain (if positive) or loss (if negative) of using $\mu_{2,3\text{-p}}$ compared to $\mu_{2\text{-p}}$. The percentage

$$g_{\text{iter}} = 100 \cdot \frac{I^*\left(\mu_{2\text{-p}}\right) - I^*\left(\mu_{2,3\text{-p}}\right)}{I^*\left(\mu_{2\text{-p}}\right)} \tag{39}$$

will show either gain (if positive) or loss (if negative) in computational speed of using $\mu_{2,3\text{-p}}$ compared to $\mu_{2\text{-p}}$.

We test both $\mu_{2\text{-p}}$ and $\mu_{2,3\text{-p}}$ for 10 to 150 ports randomly scattered. Positions of all the ports are in matrix (1), which is generated as

$$\mathbf{P} = 50 \cdot \Theta(N, 2) \tag{40}$$

by

$$N = 5 + 5n, \; n = \overline{1, 29} \tag{41}$$

and an operator $\Theta(N, 2)$ returning a pseudorandom $N \times 2$ matrix whose entries are drawn from the standard uniform distribution on the open interval (0;1). Matrix (40) is identical for both $\mu_{2\text{-p}}$ and $\mu_{2,3\text{-p}}$ in every instance, and we generate 400 such maritime cargo delivery problem instances (i. e., the test is repeated for 400 times) for every N. The maximal number of iterations is 8000, whereas the algorithm's early stop condition is used, by which (a run of) the algorithm is stopped if the shortest route length does not change for 400 iterations (a one 20th of the maximal number of iterations). The remaining parameters are:

$$M_{\max} = 16, \; \lambda = 100, \; P_{\text{merge}} = 0.15, \tag{42}$$

and

$$d_{\max} = \psi\left(\frac{1}{M_{\max}} \cdot \max_{k=\overline{1,N}} \left\{ \sum_{j=1}^{N} \rho(k, j) \right\} \right) \tag{43}$$

where function $\psi(x)$ returns the integer part of number x.

The comparison of performances of $\mu_{2\text{-p}}$ and $\mu_{2,3\text{-p}}$ is presented in Table 1, where the percentage of violations of the longest possible tour constraint (12) is shown in two separate columns for $\mu_{2\text{-p}}$ and $\mu_{2,3\text{-p}}$, regardless of whether

$$\tilde{\rho}^*_\Sigma\left(\mu_{2\text{-p}}\right) > \tilde{\rho}^*_\Sigma\left(\mu_{2,3\text{-p}}\right) \tag{44}$$

or

$$\tilde{\rho}^*_\Sigma\left(\mu_{2\text{-p}}\right) < \tilde{\rho}^*_\Sigma\left(\mu_{2,3\text{-p}}\right). \tag{45}$$

The percentage of occurrences of (44), (45) is roughly the same for $\mu_{2\text{-p}}$ and $\mu_{2,3\text{-p}}$. Every instance of 10 to 25 ports has been solved by violating the constraint. This is because the longest possible tour length (43) is relatively too short, and the maritime cargo delivery problem is likely to have no solution by such a constraint. Then, the maritime delivery service will enable one of the few feeders capable of covering longer distances, whereupon the solutions for 10 to 25 ports become feasible. For 30 to 40 ports, more than a half of the respective solutions have been revealed infeasible as well. As previously stated, the infeasibility is rectified by having less "distant" feeders: as the number of ports increases, the minimized number of feeders drops (see Table 2), and therefore the number of feeders that violate the tight constraint drops as well. The maritime cargo delivery problems of 90 ports and more have no infeasible solutions. The number of infeasible solutions for 55 to 85 ports is negligible. Moreover, considering just algorithm $\mu_{2,3\text{-p}}$, there is only 1% of the longest possible tour constraint violations for 55 ports, whereas the $\mu_{2,3\text{-p}}$-solutions to maritime cargo delivery problems of 60 ports and more are all feasible.

The computational speed is also an important property of the algorithm. Measured in the number of iterations taken to achieve a stable route (approximately the shortest length), this metric allows us to determine whether modifying the algorithm speeds up convergence. Table 3 shows the comparison of computational speeds based on (44) and (45) from Table 1, along with percentage (39).

The percentage of the longest possible tour constraint violations shown here similarly to that in Table 1 allows making complete visual comparisons. In general, if gain (38) is positive, i. e., using both the 2-point and 3-point crossover operators shortens the delivery route, algorithm $\mu_{2,3\text{-p}}$ takes up to 10% more iterations to outperform algorithm $\mu_{2\text{-p}}$ (it is over 13% for 70, 75, 90, 100, 110 ports, and it is over 16% for 55 ports). On the contrary, if using both the 2-point and 3-point crossover operators lengthens the delivery route, algorithm $\mu_{2\text{-p}}$ takes roughly between 2% to 8% more iterations to outperform algorithm $\mu_{2,3\text{-p}}$ (it is over 18% for 45 ports, and it is over 10% for 50 ports). Therefore, if we gain in the delivery route length, we may probably lose in computational speed and vice versa. Some exclusions in this test, however, exist. Thus, algorithm $\mu_{2,3\text{-p}}$ outperforms algorithm $\mu_{2\text{-p}}$ both by shortening the route length and decreasing the number of iterations for 10 and 15 ports (where every route is infeasible, though), and for 120 ports. In contrast, algorithm $\mu_{2,3\text{-p}}$ fails to shorten the route length, simultaneously increasing the number of iterations for 30 and 75 ports (where $g_{\text{iter}} < 0$ in both columns).

A typical example of the solution to the maritime cargo delivery problem of 60 ports obtained by algorithm $\mu_{2\text{-p}}$ is shown in Figure 3. Although the algorithm produces the feasible solution after 1475 iterations (not passing even a fifth part of 8000), the tour of one of the four feeders is not perfect-there is an intersection between ports 23, 11 and

43, 60, although the length of the sequence 23, 43, 11, 60 here is obviously shorter. The lengths of the feeders tours are

61.8107, 96.2493, 120.7262, 122.0094 (46)

(note that these values are rounded). The solution to this problem obtained by algorithm $\mu_{2,3\text{-p}}$ is much better (Figure 4). The algorithm produces the feasible solution after 1879 iterations (by 27.3898 % more that $\mu_{2\text{-p}}$), but the route is

Table 1. *Comparison of performances of $\mu_{2\text{-p}}$ and $\mu_{2,3\text{-p}}$ along with the percentage of violations of the longest possible tour constraint*

		$\tilde{\rho}^*_\Sigma(\mu_{2\text{-p}}) > \tilde{\rho}^*_\Sigma(\mu_{2,3\text{-p}})$				Violations of (12) in $\tilde{\rho}^*_\Sigma(\mu_{2\text{-p}})$	$\tilde{\rho}^*_\Sigma(\mu_{2\text{-p}}) < \tilde{\rho}^*_\Sigma(\mu_{2,3\text{-p}})$				Violations of (12) in $\tilde{\rho}^*_\Sigma(\mu_{2,3\text{-p}})$
		Occurrences, %	$\tilde{\rho}^*_\Sigma(\mu_{2\text{-p}})$	$\tilde{\rho}^*_\Sigma(\mu_{2,3\text{-p}})$	g		Occurrences, %	$\tilde{\rho}^*_\Sigma(\mu_{2\text{-p}})$	$\tilde{\rho}^*_\Sigma(\mu_{2,3\text{-p}})$	g	
Overall average		47.431	458.1736	439.855	4.1138	%	46.9914	437.4499	455.7348	-4.2375	%
N	10	23	162.5074	154.4293	4.9709	100	11	160.9161	168.1438	-4.4916	100
	15	36.75	245.8067	230.9942	6.026	100	31.25	224.9417	234.6612	-4.3209	100
	20	40	313.768	295.4183	5.8482	100	28.25	330.7839	343.0468	-3.7072	100
	25	51	425.7302	400.6392	5.8937	100	26.5	412.3405	428.5109	-3.9216	100
	30	57	525.7586	503.0035	4.328	98.75	36.25	486.4183	512.1281	-5.2855	98.75
	35	53.5	590.9274	573.517	2.9463	84.5	43.75	540.8242	561.0292	-3.736	84.5
	40	51	583.5659	562.5897	3.5945	59.5	49	544.3362	558.5648	-2.6139	60
	45	52	518.0818	499.4493	3.5964	27.75	48	474.4119	491.0923	-3.516	28.5
	50	52	454.3131	433.8998	4.4932	12.5	48	446.6779	469.3174	-5.0684	10.75
	55	49.75	429.9538	413.2041	3.8957	1	50.25	415.2039	436.668	-5.1695	1
	60	47	426.2364	408.5017	4.1608	0	53	397.0233	421.1186	-6.069	0
	65	47.5	427.1261	407.691	4.5502	0	52.5	402.2233	422.0906	-4.9394	0
	70	50.5	422.2514	404.6076	4.1785	0.25	49.5	405.5613	426.0908	-5.062	0
	75	39	428.1851	404.5786	5.5132	0.25	61	410.862	429.2739	-4.4813	0
	80	47.75	436.9097	421.5664	3.5118	0	52.25	409.9417	431.4875	-5.2558	0
	85	46.75	444.7619	427.6235	3.8534	0.5	53.25	431.4437	448.2362	-3.8922	0
	90	49.75	452.3774	434.3581	3.9832	0	50.25	433.1648	452.6187	-4.4911	0
	95	45.75	455.9687	437.1885	4.1187	0	54.25	435.0251	457.0975	-5.0738	0
	100	55.75	470.2506	448.7076	4.5812	0	44.25	443.5044	462.9149	-4.3766	0
	105	50	468.1526	452.0036	3.4495	0	50	450.2579	470.5579	-4.5085	0
	110	48.75	478.6923	459.2945	4.0523	0	51.25	460.0941	481.9455	-4.7493	0
	115	44	483.7243	470.5481	2.7239	0	56	470.3821	488.3825	-3.8268	0
	120	48.5	494.7954	476.7706	3.6429	0	51.5	475.815	490.2046	-3.0242	0
	125	44.5	507.5657	487.6522	3.9233	0	55.5	483.5862	500.2591	-3.4477	0
	130	53.25	512.0419	493.1712	3.6854	0	46.75	492.2423	512.2915	-4.073	0
	135	41	520.7821	499.6678	4.0543	0	59	501.1695	515.4461	-2.8487	0
	140	60.75	522.946	506.7323	3.1005	0	39.25	503.2026	524.0261	-4.1382	0
	145	37.75	537.827	518.1812	3.6528	0	62.25	515.1312	535.2688	-3.9092	0
	150	51.25	546.0285	529.8046	2.9712	0	48.75	528.5614	543.8372	-2.8901	0

Table 2. *The average number of feeders M* by* $\mu_{2\text{-p}}$ *and* $\mu_{2,3\text{-p}}$

N	10	15	20	25	30	35	40	45	50	55
M^* by $\mu_{2\text{-p}}$	2.42	4.09	5.3875	6.7525	7.5375	7.655	6.98	5.66	4.7	4.1325
M^* by $\mu_{2,3\text{-p}}$	2.32	3.9325	5.275	6.6	7.4975	7.64	6.9175	5.64	4.6925	4.1775
N	60	65	70	75	80	85	90	95	100	105
M^* by $\mu_{2\text{-p}}$	3.6325	3.5225	3.16	3.045	3.0175	2.9725	2.96	2.775	2.6925	2.4025
M^* by $\mu_{2,3\text{-p}}$	3.74	3.44	3.19	3.045	3.0025	2.995	2.9475	2.8125	2.62	2.42
N	110	115	120	125	130	135	140	145	150	
M^* by $\mu_{2\text{-p}}$	2.305	2.1375	2.095	2.0325	2	2.0225	2	2	2	
M^* by $\mu_{2,3\text{-p}}$	2.3425	2.18	2.07	2.0525	2	2.02	2	2.025	2	

5.1186 % shorter. Besides, the shorter route consists of three feeders whose tour lengths are

120.2504, 132.2812, and 127.7488 (47)

being roughly equal and not much longer than the longest tour in (46). This means that the maritime delivery service, apart from the shorter route in Figure 4, spares here a feeder. Moreover, the lengths of the four feeders tours (46) are more unequal than the lengths (47). This additionally rationalizes the occupation of the three feeders.

As the longest possible tour constraint (12) is made looser, i. e. the longest possible tour length becomes not so short, the percentage of violations of constraint (12) in both $\mu_{2\text{-p}}$ and $\mu_{2,3\text{-p}}$ becomes significantly lower even for a few tens of ports. Thus, if

$$d_{\max} = \psi\left(\frac{3}{M_{\max}} \cdot \max_{k=1,N}\left\{\sum_{j=1}^{N} \rho(k,j)\right\}\right) \tag{48}$$

instead of (43), then this violation rate is about 50 % for 15 ports, but it is 0 for 20 ports or more. The percentage of occurrences of (44), (45) is still roughly the same for $\mu_{2\text{-p}}$ and $\mu_{2,3\text{-p}}$, although the occurrence of (44) is a little bit more probable (just it is in Table 1). The violation rate by (48) for 10 ports is less than 100%, but it is not less than 90 %. If

$$d_{\max} = \psi\left(\frac{6}{M_{\max}} \cdot \max_{k=1,N}\left\{\sum_{j=1}^{N} \rho(k,j)\right\}\right) \tag{49}$$

then there are almost no violations for 15 and 10 ports. Furthermore, it is much more probable at (49) that the gain by (38) will appear positive.

Consequently, half of routes could be made shorter while the 2-point crossover operator is solely used. On the contrary, half of routes could also be made shorter while both the 2-point and 3-point crossover operators are solely used (embedded in the corresponding algorithm $\mu_{2,3\text{-p}}$). The best decision here is to run both $\mu_{2\text{-p}}$ and $\mu_{2,3\text{-p}}$ simultaneously (in parallel), whereupon the shortest route length is

$$\tilde{\rho}_{\Sigma}^{**} = \min\left\{\tilde{\rho}_{\Sigma}^{*}\left(\mu_{2\text{-p}}\right), \tilde{\rho}_{\Sigma}^{*}\left(\mu_{2,3\text{-p}}\right)\right\} \tag{50}$$

and the respective route is selected according to (50).

7. Discussion of the Contribution

Our contribution to the field of genetic algorithms consists in the suggested 3-point crossover operation over three chromosomes followed by a confluence with 2-point crossover mutations and a two-branched algorithm to obtain the shortest route length (50). This two-branched algorithm does not have practical limitations unless the maximal number of available feeders is 2. The practical applicability and significance of the suggested crossover mutation operation (involving both 2-point and 3-point crossover mutations) can be illustrated by an example generated for 15 ports by (49) implying a looser longest possible tour constraint (Figure 5). The longest possible tour length is 186. The route by $\mu_{2\text{-p}}$ whose length is $\tilde{\rho}_{\Sigma}^{*}(\mu_{2\text{-p}})$ = 211.6745 consists of two feeders tours whose lengths are 135.2037 and 76.4708. The route by $\mu_{2,3\text{-p}}$ whose length is $\tilde{\rho}_{\Sigma}^{*}(\mu_{2\text{-p}})$ = 183.4649 consists of a single feeder tour. Therefore, the maritime delivery service, apart from the 15.376 % shorter route, spares here a feeder. It is noteworthy that these results are obtained by $I^*(\mu_{2\text{-p}})$ = 482 and $I^*(\mu_{2,3\text{-p}})$ = 454 (by the maximum of 8000 iterations and the early stop condition of 400 iterations). Amazingly enough, the same results are obtained by setting the maximum at 800 iterations and the early stop condition at 40 iterations, where $I^*(\mu_{2\text{-p}})$ = 122 and $I^*(\mu_{2,3\text{-p}})$ = 94 (the difference between the past iterations is the same). The gains in Table 1 are noticeably less than the gain in this example, but Table 1 shows the results of the worst-case scenario when the longest possible tour constraint (12) is very tight, as given by (43). It is expected

Table 3. *Computational speed of $\mu_{2\text{-}p}$ and $\mu_{2,3\text{-}p}$ compared by Table 1*

		$\tilde{\rho}^*_\Sigma(\mu_{2\text{-}p}) > \tilde{\rho}^*_\Sigma(\mu_{2,3\text{-}p})$			Violations of (12) in $\tilde{\rho}^*_\Sigma(\mu_{2\text{-}p})$	$\tilde{\rho}^*_\Sigma(\mu_{2\text{-}p}) < \tilde{\rho}^*_\Sigma(\mu_{2,3\text{-}p})$			Violations of (12) in $\tilde{\rho}^*_\Sigma(\mu_{2,3\text{-}p})$
		$I^*(\mu_{2\text{-}p})$	$I^*(\mu_{2,3\text{-}p})$	g_{iter}		$I^*(\mu_{2\text{-}p})$	$I^*(\mu_{2,3\text{-}p})$	g_{iter}	
Overall average		2697.546	2901.208	-7.4452	%	2946.626	2770.845	5.3356	%
N	**10**	**455.3043**	**445.75**	**2.0985**	100	**448.8182**	**429.6591**	**4.2688**	100
	15	**504.2177**	**469.034**	**6.9779**	100	**514.432**	**465.312**	**9.5484**	100
	20	559.3563	578.4125	-3.4068	100	559.928	534.736	4.4991	100
	25	654.0049	693.3627	-6.018	100	667.056	664.92	0.3202	100
	30	819.2763	869.0132	-6.0708	98.75	864.2414	995.4828	-15.1857	98.75
	35	1065.969	1195.921	-12.1909	84.5	1134.354	1105.817	2.5157	84.5
	40	1376.004	1440.702	-4.7018	59.5	1524.194	1395.393	8.4504	60
	45	1510.132	1677.746	-11.0993	27.75	1888.138	1544	18.2263	28.5
	50	1761.965	1827.675	-3.7294	12.5	2134.174	1920.245	10.024	10.75
	55	1812.197	2113.233	-16.6116	1	2122.134	2007.119	5.4198	1
	60	1853.048	2064.561	-11.4143	0	2367.212	2183.637	7.7549	0
	65	2181.851	2410.127	-10.4625	0	2461.028	2287.552	7.0489	0
	70	2224.693	2532.825	-13.8505	0.25	2658.274	2461.274	7.4108	0
	75	2284.838	2598.961	-13.7481	0.25	2659.676	2739.721	-3.0096	0
	80	2653.943	2814.316	-6.0428	0	2894.164	2685.094	7.2238	0
	85	2722.597	3006.794	-10.4385	0.5	3114.459	2952.709	5.1935	0
	90	2883.697	3291	-14.1243	0	3146.791	3064.135	2.6267	0
	95	2996.233	3324.325	-10.9502	0	3447.094	3312.103	3.9161	0
	100	3335.43	3772.412	-13.1012	0	3647.566	3520.439	3.4853	0
	105	3648.702	3968.754	-8.7717	0	3831.799	3558.123	7.1422	0
	110	3652.281	4178.803	-14.4163	0	4032.844	4017.762	0.374	0
	115	4049.925	4203.404	-3.7897	0	4182.348	3811.094	8.8767	0
	120	**4269.557**	**4251.351**	**0.4264**	0	**4543.357**	**4164.734**	**8.3336**	0
	125	4130.184	4443.36	-7.5826	0	4535.119	4336.525	4.379	0
	130	4586.281	4767.798	-3.9578	0	4677.566	4284.959	8.3934	0
	135	4792.899	4928.614	-2.8316	0	4870.484	4669.73	4.1219	0
	140	4957.222	5220.527	-5.3115	0	5216.717	4776.971	8.4296	0
	145	5090.86	5475.712	-7.5597	0	5583.249	5081.49	8.9869	0
	150	5396.156	5570.547	-3.2318	0	5724.94	5383.783	5.9591	0

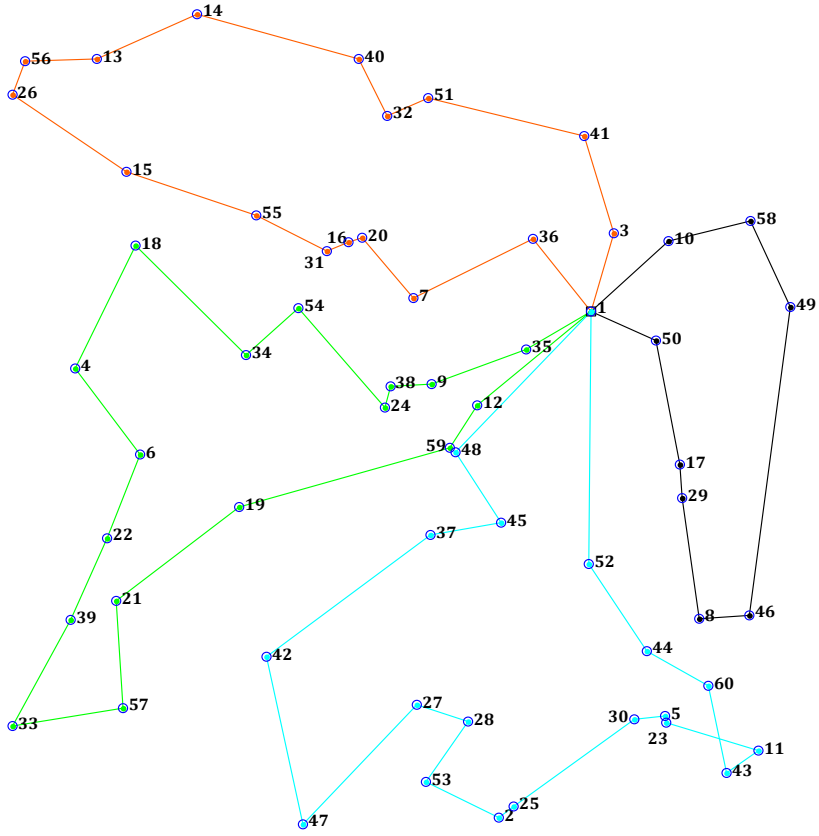

Figure 3. *The solution of an instance with 60 ports by* $\mu_{2\text{-}p}$*, where four feeders are used and* $\tilde{p}_{\Sigma}^{*} = 400.7957$

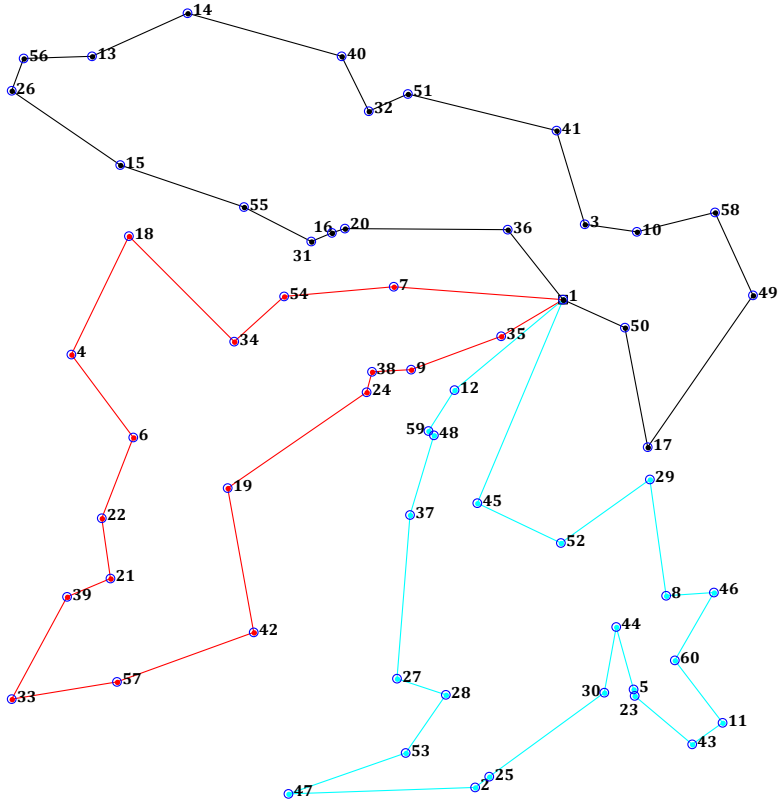

Figure 4. *A better solution of the instance with 60 ports in Figure 3 by* $\mu_{2,3\text{-}p}$*, where three feeders are used and* $\tilde{p}_{\Sigma}^{*} = 380.2804$

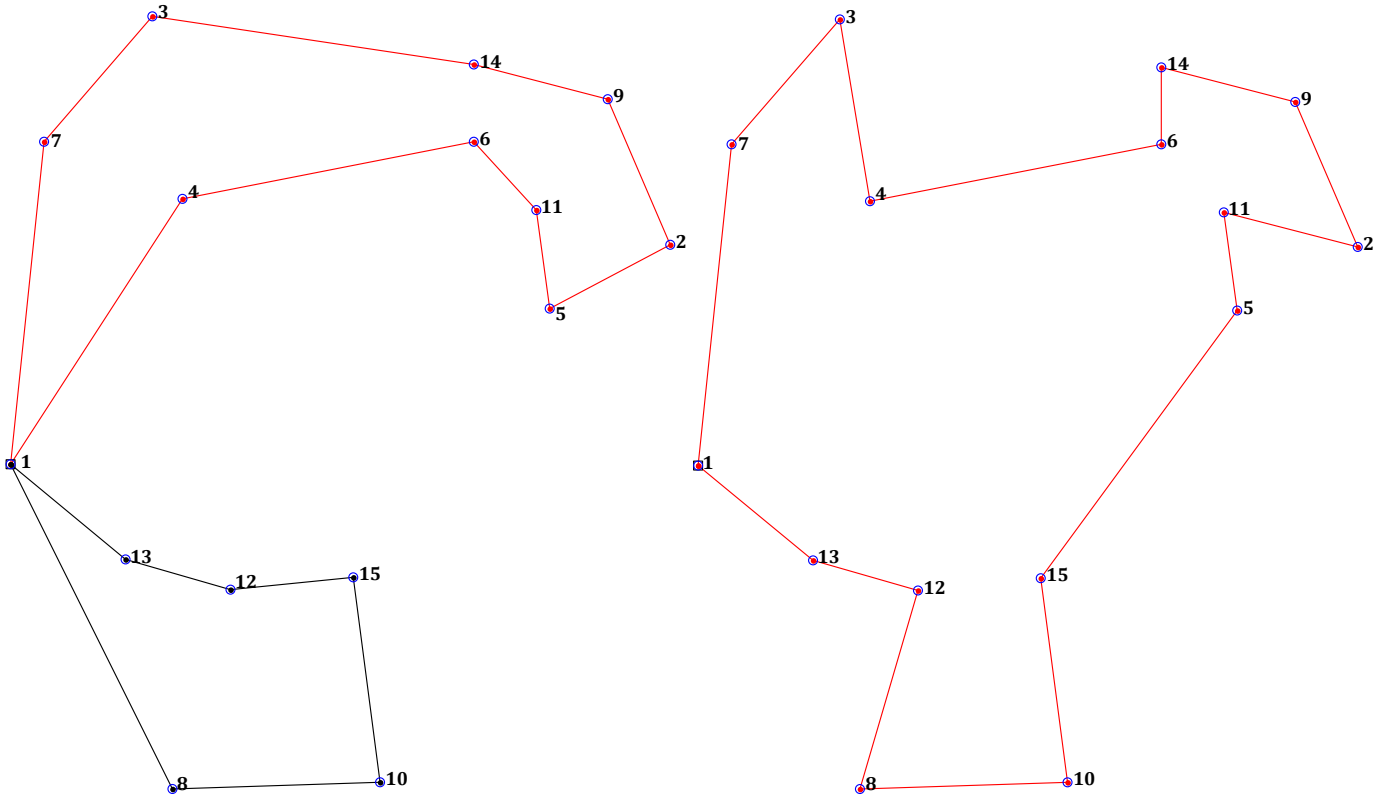

Figure 5. *The route by $\mu_{2\text{-}p}$ (left) shortened by 15.376 % by using $\mu_{2,3\text{-}p}$ (the route at the right)*

that the gain can be very significant if the constraint is looser, whether there are 10 ports or a few tens and more.

Along with minimizing the route length, the algorithm runs with the effect of the indirect minimization of the number of feeders. This is another side of maritime cargo delivery optimization, as maintenance of the feeder fleet is much more expensive. If the route consists of one or a few too-short feeders tours, then some tours may be accomplished by the same feeder (while some other feeder is accomplishing its longer tour), but this decision is made only by the maritime delivery service.

It is necessary to mention that, despite our model of delivering cargo is very simple, it reflects the delivery core-distance and capacity (capability). We also based our research on the fact that the positions of the ports are generated normally. This might be a tiny bias because, in reality, a maritime delivery service may be contracted to deliver from its hub to neighboring and distant ports that, in the aggregate, would not look like the center-based cluster shown in Figure 3 (Figure 4). However, we believe that this drawback is counterbalanced by our worst-case scenario consideration.

Another seeming deterrent is the computational speed that has been not improved. Indeed, algorithm $\mu_{2,3\text{-}p}$ does not converge faster. Nevertheless, running both algorithms $\mu_{2\text{-}p}$ and $\mu_{2,3\text{-}p}$ in parallel is strongly recommended (and it is perfectly possible using methods of parallelization of computing). Consequently, with paying attention back to Table 3, the computational speed herein is not slowed down.

8. Conclusion

We have presented a 3-point crossover operator to the genetic algorithm for solving a maritime cargo delivery problem formulated as a multiple traveling salesman problem. This operator returns slightly more complex crossover mutations, which in the confluence with 2-point crossover mutations shorten the delivery route in about 50% of algorithm runs. However, this 2-point-and-3-point crossover algorithm does not shorten every route. To definitely increase the genetic algorithm performance, we have proposed to run both the 2-point crossover algorithm and the 2-point-and-3-point crossover algorithm in parallel and select the minimal length route. The route may be shortened by a few percentage points, but the resulting cost savings for maritime cargo delivery are substantial.

Therefore, it is a significant contribution to the field of genetic algorithms, which are specifically used to optimize maritime cargo delivery. The impact of our contribution is obvious for policymakers and practitioners: the rationalization of maritime transportation route planning saves energy (fuel for ship feeders is saved), transport (feeders themselves are spared), and human (fewer seamen and service personnel are needed) resources.

Potential development of the research would be to test more complex mutations, including combinations of flip, swap, and slide, in addition to "pure" crossover [18]. We believe that complicated mutations may be acceptable if the mutated part of the chromosome is relatively small (i. e., the mutated chromosome is still "recognizable" compared to its parents). The question of how the mutation diversity influences algorithm convergence and the indirect minimization of the number of feeders is still open. Reducing this number and the equalization of the lengths of feeders tours do lead to an additional reduction in the cost of maritime cargo delivery.

Peer-review: Externally and internally peer-reviewed.

Authorship Contributions

Concept design: M.O. Malaksiano, Data Collection or Processing: A.Y. Romanov, Analysis or Interpretation: V.V. Romanuke, Literature Review: A.Y. Romanov, M.O. Malaksiano, Writing, Reviewing and Editing: V.V. Romanuke.

Funding: The author(s) received no financial support for the research, authorship, and/or publication of this article.

References

[1] "Global cargo shipping market." [Online]. Available: https://www.databridgemarketresearch.com/reports/global-cargo-shipping-market. [Accessed: May 6, 2022].

[2] Review of Maritime Transport 2019, *United Nations Conference on Trade and Development*. Geneva: United Nations, 2020. [Online]. Available: https://unctad.org/en/PublicationsLibrary/rmt2019_en.pdf. [Accessed: May 6, 2022].

[3] "What is PESTLE analysis? An important business analysis tool." [Online]. Available: https://pestleanalysis.com/what-is-pestle-analysis/amp. [Accessed: May 6, 2022].

[4] "Cargo shipping market." [Online]. Available: https://www.fortunebusinessinsights.com/cargo-shipping-market-102045. [Accessed: May 8, 2022].

[5] "Logistics solutions." [Online]. Available: https://www.maersk.com. [Accessed: May 8, 2022].

[6] "A leader in shipping & logistics." [Online]. Available: https://www.msc.com. [Accessed: May 8, 2022].

[7] "A world leading container fleet, a service network with disruption-free global coverage." [Online]. Available: https://lines.coscoshipping.com/home. [Accessed: May 10, 2022].

[8] "What are your needs? We operate in over 160 countries through 755 agencies, we design and implement intelligent solutions to take care of your cargo right across the supply chain." [Online]. Available: https://www.cma-cgm.com. [Accessed: May 10, 2022].

[9] C. Archetti, L. Peirano, and M.G. Speranza, "Optimization in multimodal freight transportation problems: A Survey," *European Journal of Operational Research*, vol. 299, pp. 1-20, May 2022.

[10] P.A. Miranda, C.A. Blazquez, C. Obreque, J. Maturana-Ross, and G. Gutierrez-Jarpa, "The bi-objective insular traveling salesman problem with maritime and ground transportation costs," *European Journal of Operational Research*, vol. 271, pp. 1014-1036, Dec 2018.

[11] O. Cheikhrouhou, and I. Khouf, "A comprehensive survey on the Multiple Traveling Salesman Problem: Applications, approaches and taxonomy," *Computer Science Review*, vol. 40, Article ID 100369, May 2021.

[12] S. Sofianopoulou, and I. Mitsopoulos, "A review and classification of heuristic algorithms for the inventory routing problem," *International Journal of Operational Research*, vol. 41, pp. 282-298, June 2021.

[13] N. Cabrera, J.-F. Cordeau, and J.E. Mendoza, "The doubly open park-and-loop routing problem," *Computers & Operations Research*, vol. 143, Article ID 105761, July 2022.

[14] D.-Z. Du, and P.M. Pardalos, *Handbook of Combinatorial Optimization*. New York, NY, USA: Springer, 1998.

[15] A. Hertz, and M. Widmer, "Guidelines for the use of meta-heuristics in combinatorial optimization," *European Journal of Operational Research*, vol. 151, pp. 247-252, Dec 2003.

[16] A. Colorni, M. Dorigo, F. Maffioli, V. Maniezzo, G. Righini, and M. Trubian, "Heuristics from nature for hard combinatorial optimization problems," *International Transactions in Operational Research*, vol. 3, pp. 1-21, Jan 1996.

[17] L.D. Chambers, *The Practical Handbook of Genetic Algorithms*. Chapman and Hall/CRC, Dec 2000.

[18] R.L. Haupt, and S.E. Haupt, *Practical Genetic Algorithms*. John Wiley & Sons, 2003.

[19] L. Kota, and K. Jarmai, "Mathematical modeling of multiple tour multiple traveling salesman problem using evolutionary programming," *Applied Mathematical Modelling*, vol. 39, pp. 3410-3433, June 2015.

[20] A. Király, and J. Abonyi, "Redesign of the supply of mobile mechanics based on a novel genetic optimization algorithm using Google Maps API," *Engineering Applications of Artificial Intelligence*, vol. 38, pp. 122-130, Feb 2015.

[21] A. Shafiee, M. Arab, Z. Lai, Z. Liu, and A. Abbas, "Automated process flowsheet synthesis for membrane processes using genetic algorithm: role of crossover operators," in *Computer Aided Chemical Engineering*, vol. 38, Z. Kravanja and M. Bogataj, Eds. Elsevier, 2016, pp. 1201-1206.